Methods to measure the cosmic-ray composition with the Auger Engineering Radio Array

Fabrizia Canfora

NNV 2018

Nikhef

Radboud Universiteit Nijmegen

PIERRE AUGER OBSERVATORY

AERA Auger Engineering Radio Array

Outline

- Ultra-high-energy cosmic rays and extensive air showers
- Radio emission from extensive air showers
- Pierre Auger Observatory & Auger Engineering Radio Array
- Cosmic-ray composition techniques based on radio detection

Ultra-high-energy cosmic rays

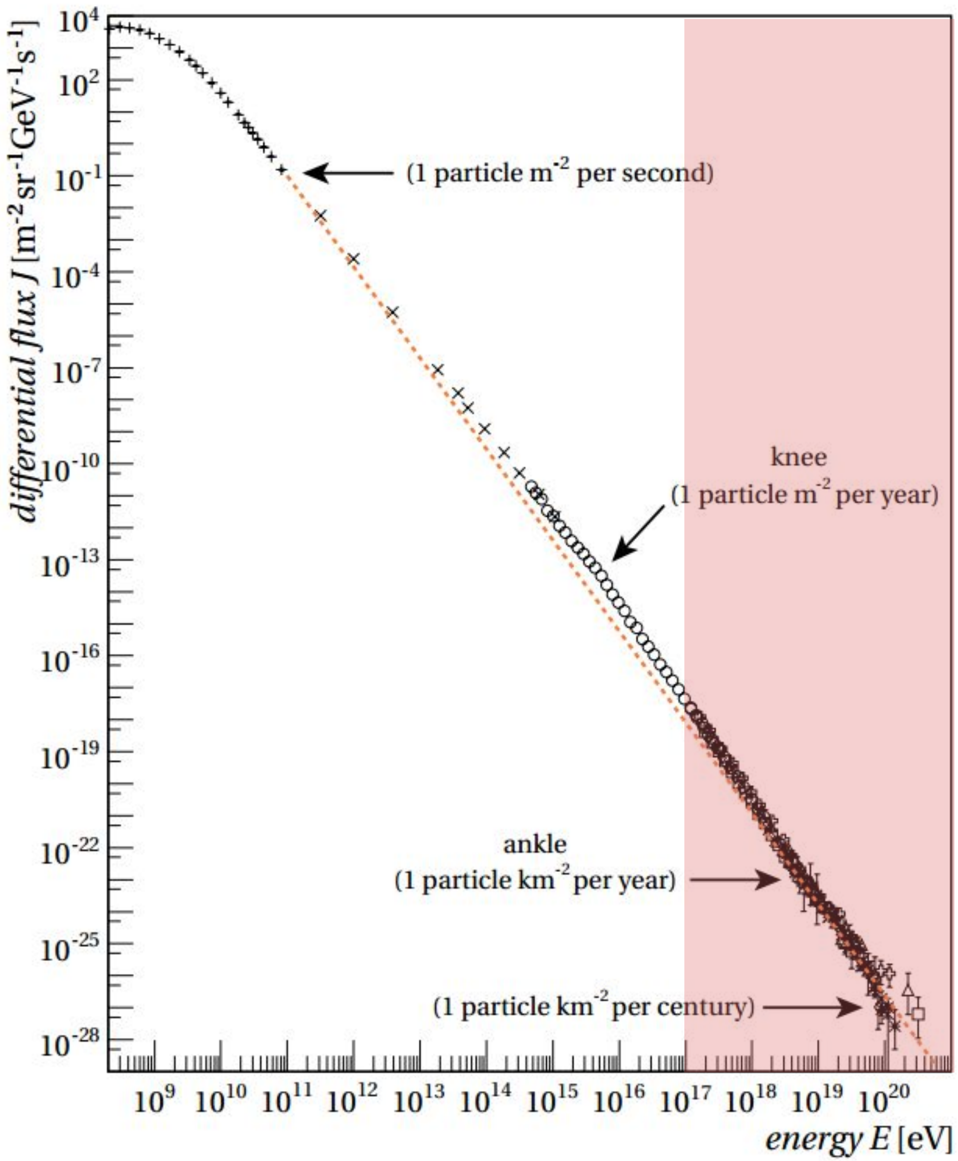

Ultra-high-energy cosmic rays
1 particle km^{-2} per century→
Large area detector

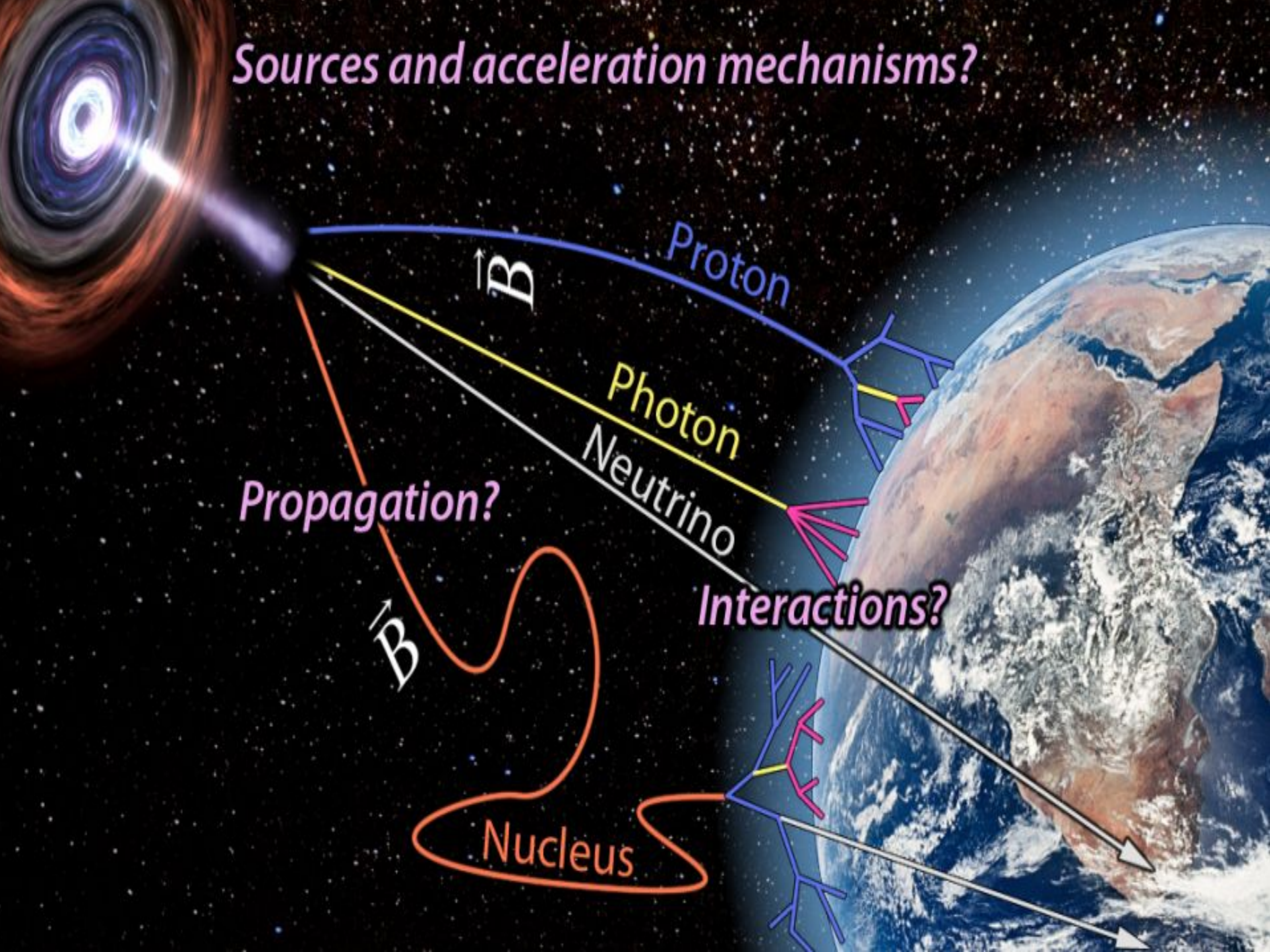
Sources and acceleration mechanisms?
$\vec{B}$
Proton
Photon
Neutrino
Propagation?
Interactions?
$\vec{B}$
Nucleus

Extensive air shower

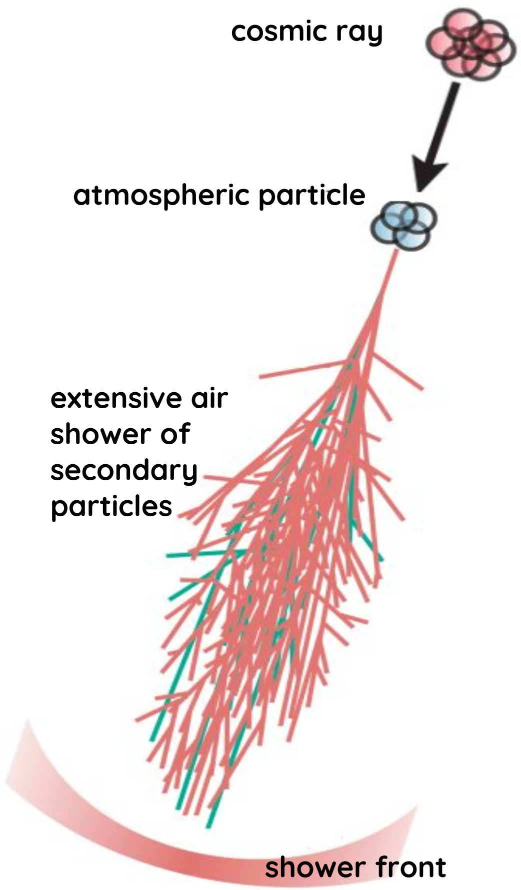

Primary particle?
Mass?
Charge?
Energy?
Arrival direction?

Fluorescence light

Secondary particles at ground level

Radio signals

Radio emission from extensive air showers

- **Geomagnetic:**
  - e^+ and e^- separation in the Earth magnetic field
  - radiation linearly polarized in the direction of the Lorentz force

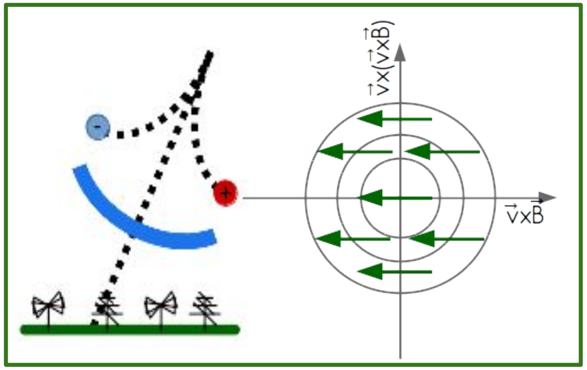

- **Charge excess:**
  - longitudinal charge imbalance
  - radiation radially polarized towards the shower axis

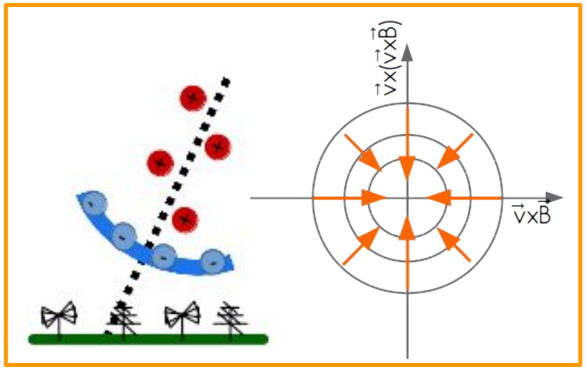

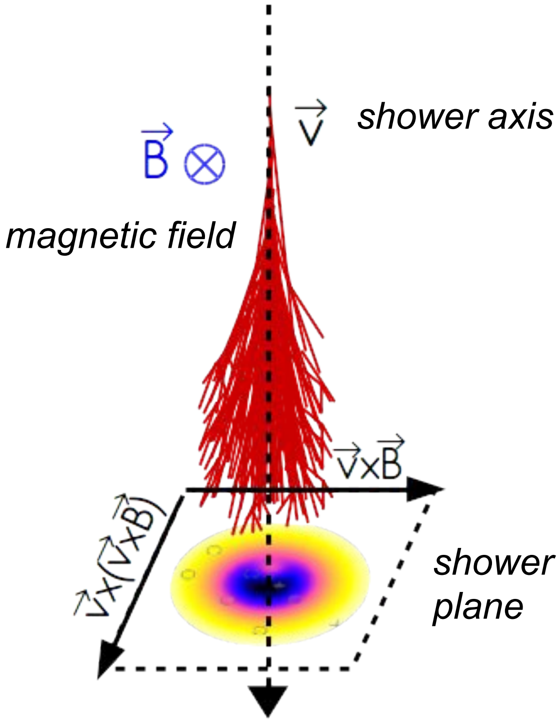

Radio emission from extensive air showers

- **Geomagnetic:**
  - e^+ and e^- separation in the Earth magnetic field
  - radiation linearly polarized in the direction of the Lorentz force

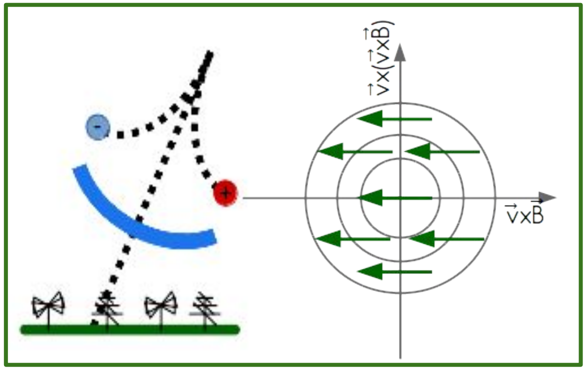

- **Charge excess:**
  - longitudinal charge imbalance
  - radiation radially polarized towards the shower axis

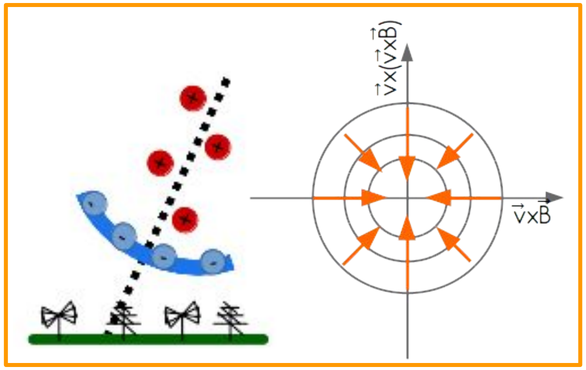

Asymmetric footprint

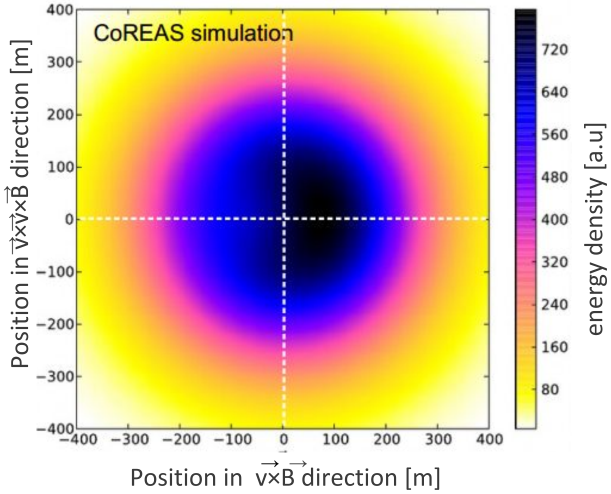

Ultra-high-energy cosmic rays Detector

Sensitive to cosmic rays above 10^{17} eV

Located in the Argentinean pampa

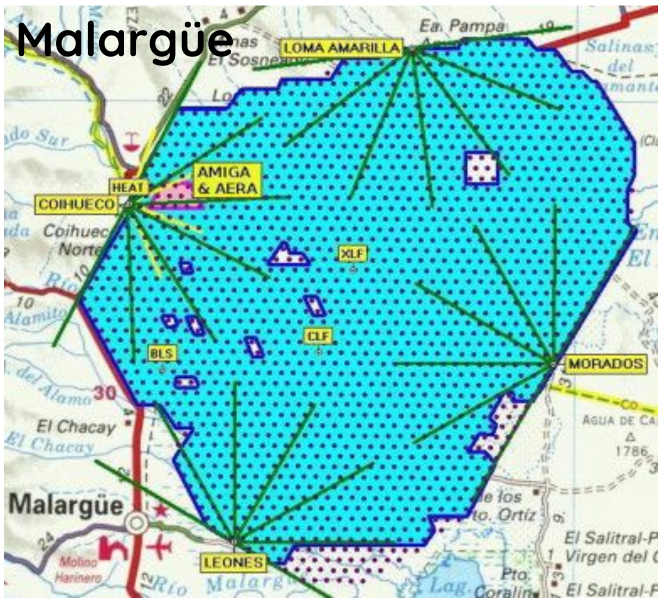

Surface area of about 3000 km^2
~ 30 times Paris

Hybrid detector: combine independent detection methods

- **27** fluorescence telescopes (FD)
- **1660** particle detectors (SD)
- **153** antennas for radio detection (Auger Engineering Radio Array) ~17 km^2

Ultra-high-energy cosmic rays Detector

Sensitive to cosmic rays above 10^{17} eV

Located in the Argentinean pampa

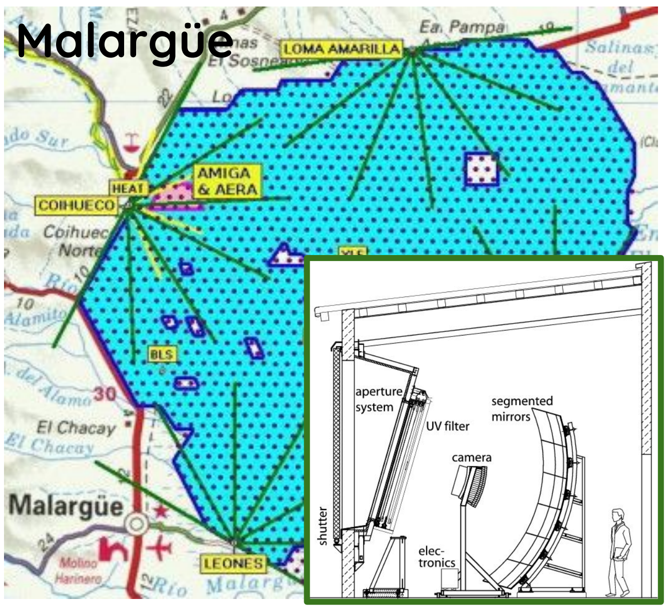

Hybrid detector: combine independent detection methods

- **27** fluorescence telescopes (FD)
- **1660** particle detectors (SD)
- **153** antennas for radio detection (Auger Engineering Radio Array) ~17 km^2

Surface area of about 3000 km^2
~ 30 times Paris

The Pierre Auger Observatory

Ultra-high-energy cosmic rays Detector

Sensitive to cosmic rays above 10^{17} eV

Located in the Argentinean pampa

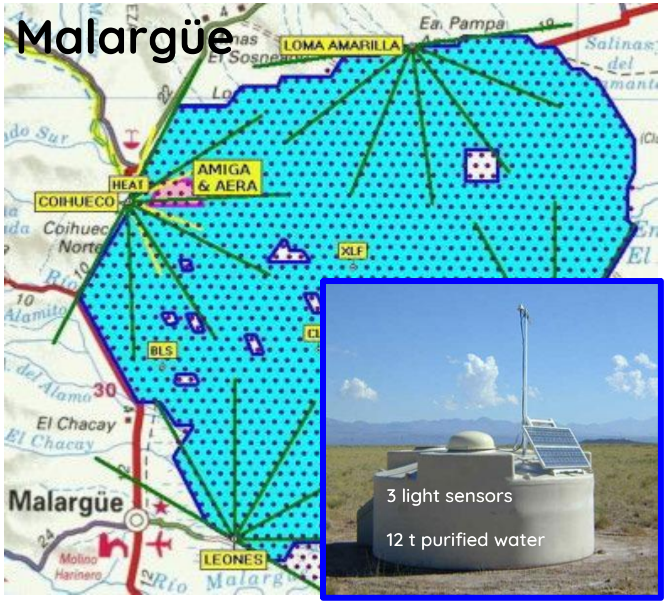

Surface area of about 3000 km^2
~ 30 times Paris

Hybrid detector: combine independent detection methods

- 27 fluorescence telescopes (FD)

- 1660 particle detectors (SD)

- 153 antennas for radio detection (Auger Engineering Radio Array) ~17 km^2

The Pierre Auger Observatory

Ultra-high-energy cosmic rays Detector

Sensitive to cosmic rays above 10^{17} eV

Located in the Argentinean pampa

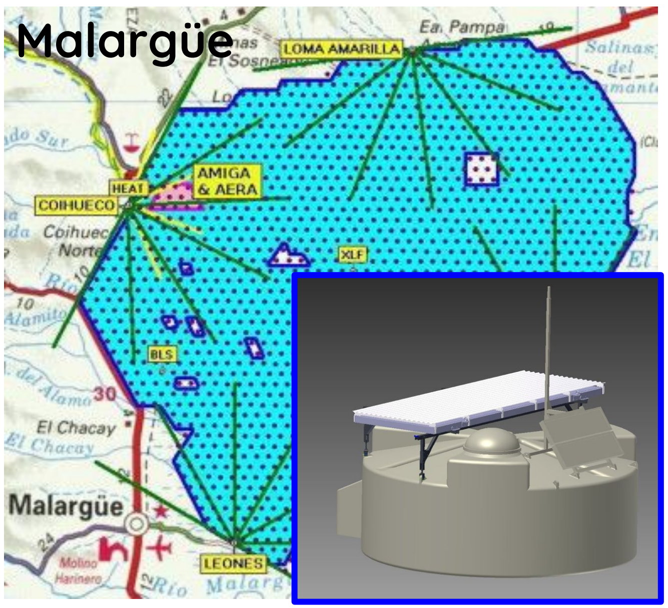

Surface area of about 3000 km^2

~ 30 times Paris

Hybrid detector: combine independent detection methods

- 27 fluorescence telescopes (FD)

- **1660** particle detectors (SD) + Scintillator Surface Detector (SSD) (Auger Upgrade)

- **153** antennas for radio detection (Auger Engineering Radio Array) ~17 km^2

The Pierre Auger Observatory

Ultra-high-energy cosmic rays Detector
Sensitive to cosmic rays above 10^{17} eV

Located in the Argentinean pampa

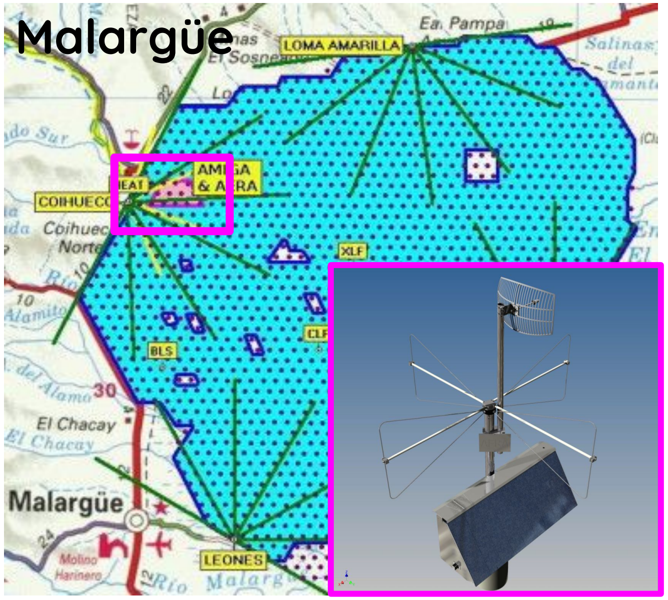

Surface area of about 3000 km^2
~ 30 times Paris

Hybrid detector: combine independent detection methods

- 27 fluorescence telescopes (FD)
- 1660 particle detectors (SD)
- 153 antennas for radio detection (Auger Engineering Radio Array) ~17 km^2

The Pierre Auger Observatory

Ultra-high-energy cosmic rays Detector

Sensitive to cosmic rays above 10^{17} eV

Located in the Argentinean pampa

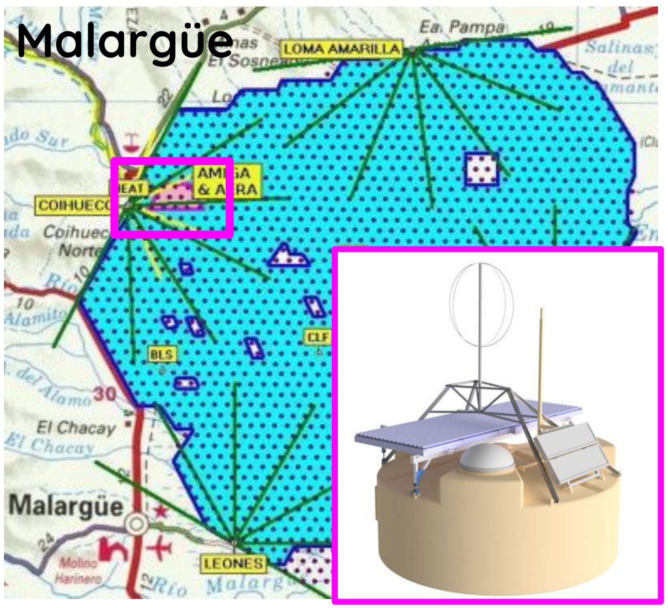

Surface area of about 3000 km^2

~ 30 times Paris

Hybrid detector: combine independent detection methods

- 27 fluorescence telescopes (FD)

- 1660 particle detectors (SD)

- 153 antennas for radio detection (Auger Engineering Radio Array) ~17 km^2 + antenna on top of each particle detector → 1660 antennas (Auger Upgrade)

Lighter nuclei interact deeper in the atmosphere

X_{max} atmospheric depth where the number of charged particles is the largest

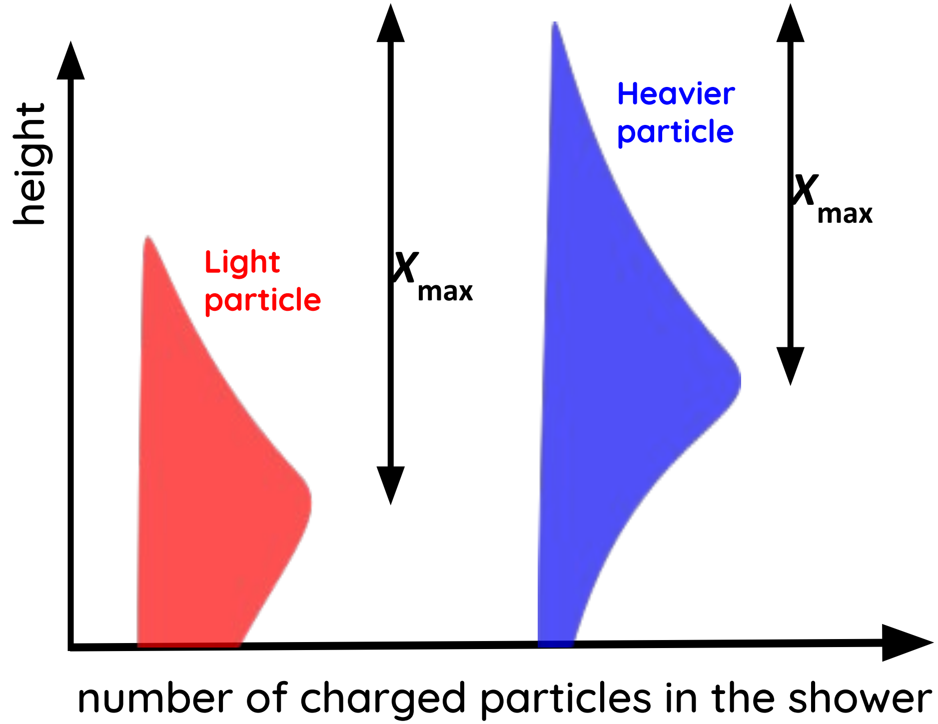

FD measurements

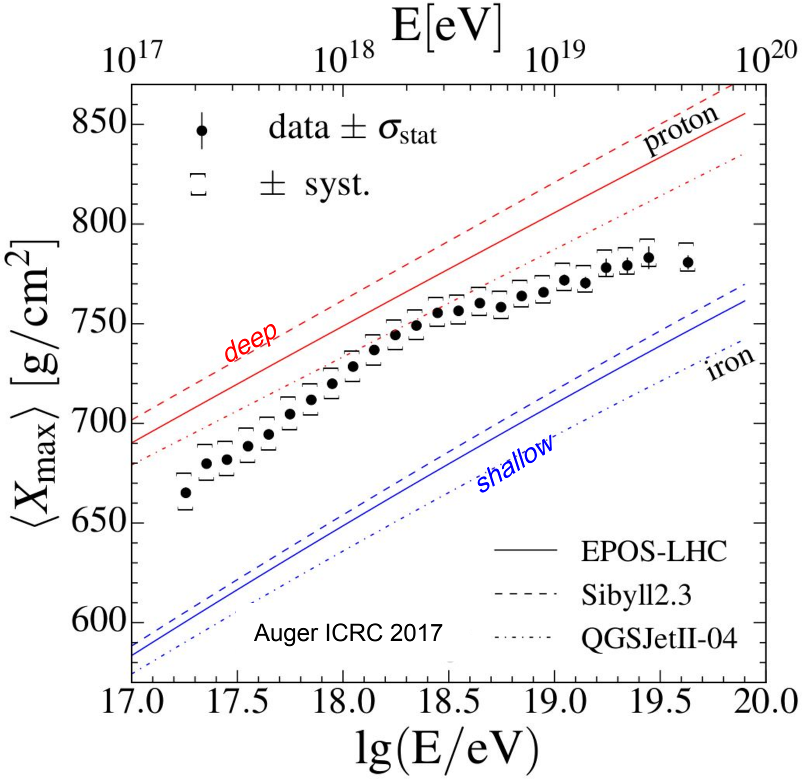

Xmax from the radio signal

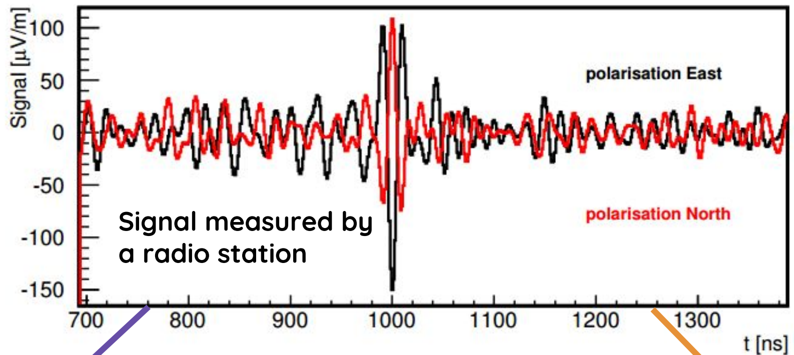

Peak of signal

Fourier Transformation

1. X_{max} from the energy density footprint

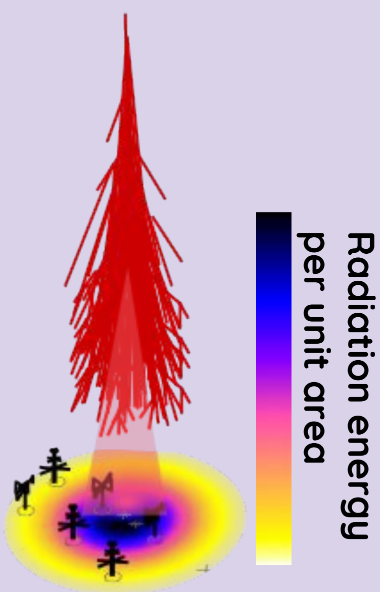

2. X_{max} from spectral information

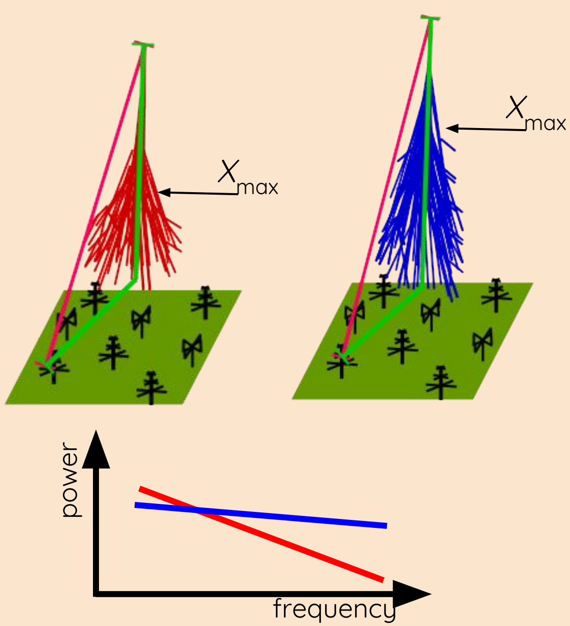

Xmax from the energy density footprint

1.

Parametrization of the energy density distribution:

description of the geomagnetic and charge excess mechanisms

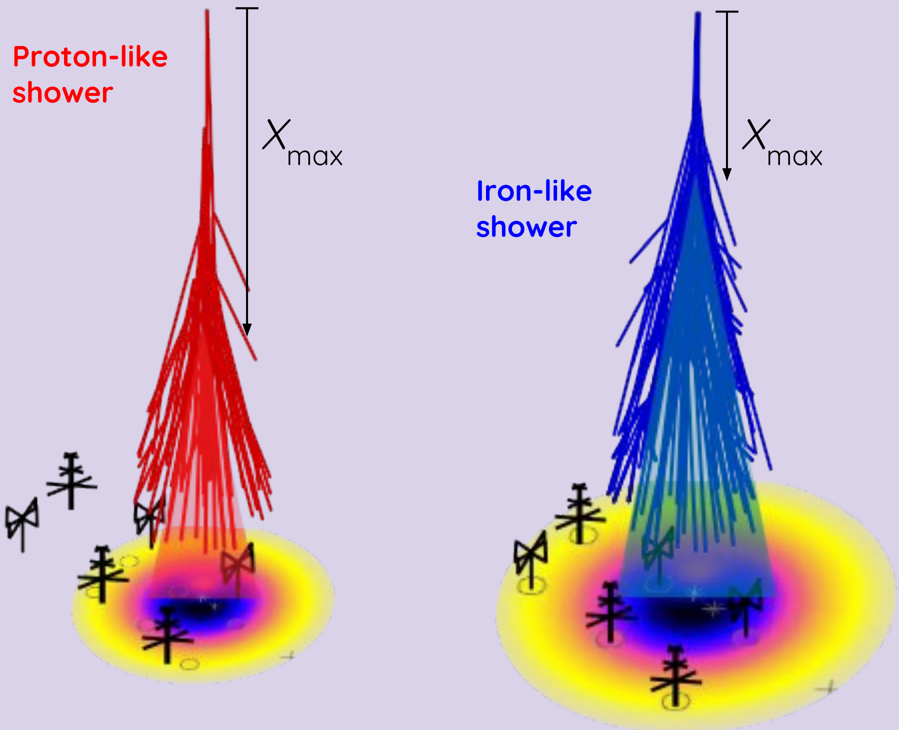

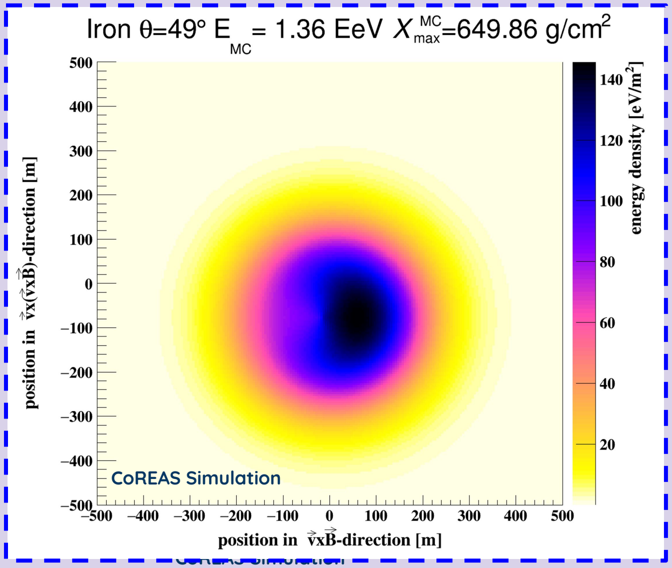

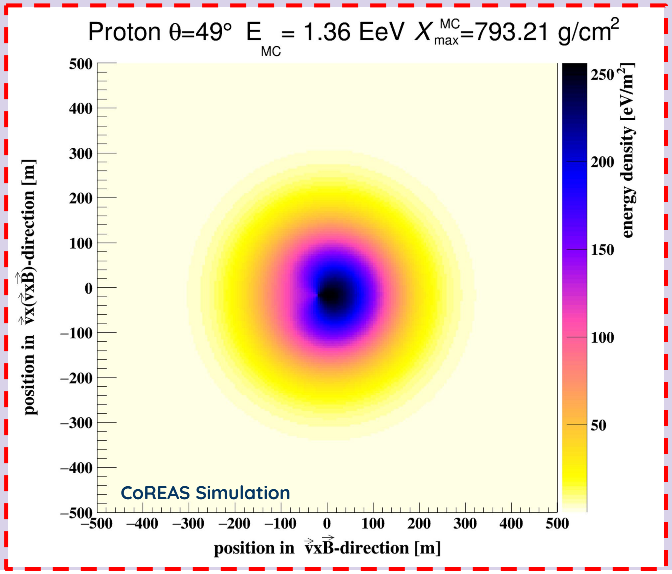

Xmax from the energy density footprint

1

Parametrization of the energy density distribution:

description of the geomagnetic and charge excess mechanisms

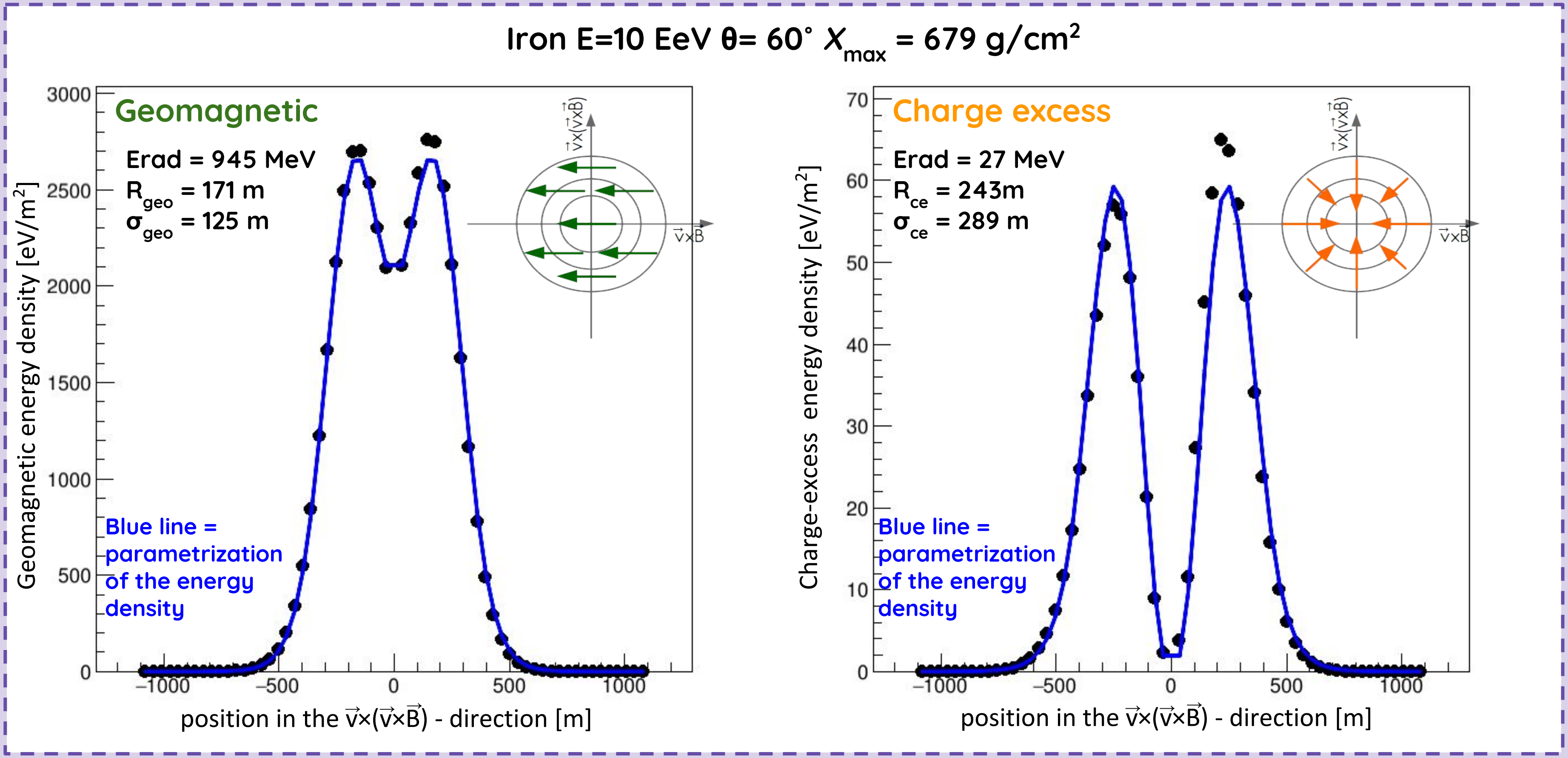

CoREAS simulation with a star-shaped antenna alignment in the shower plane $\vec{v}\times\vec{B}$-$\vec{v}\times\vec{v}\times\vec{B}$

Xmax from the energy density footprint

1

Parametrization of the energy density distribution:

description of the geomagnetic and charge excess mechanisms

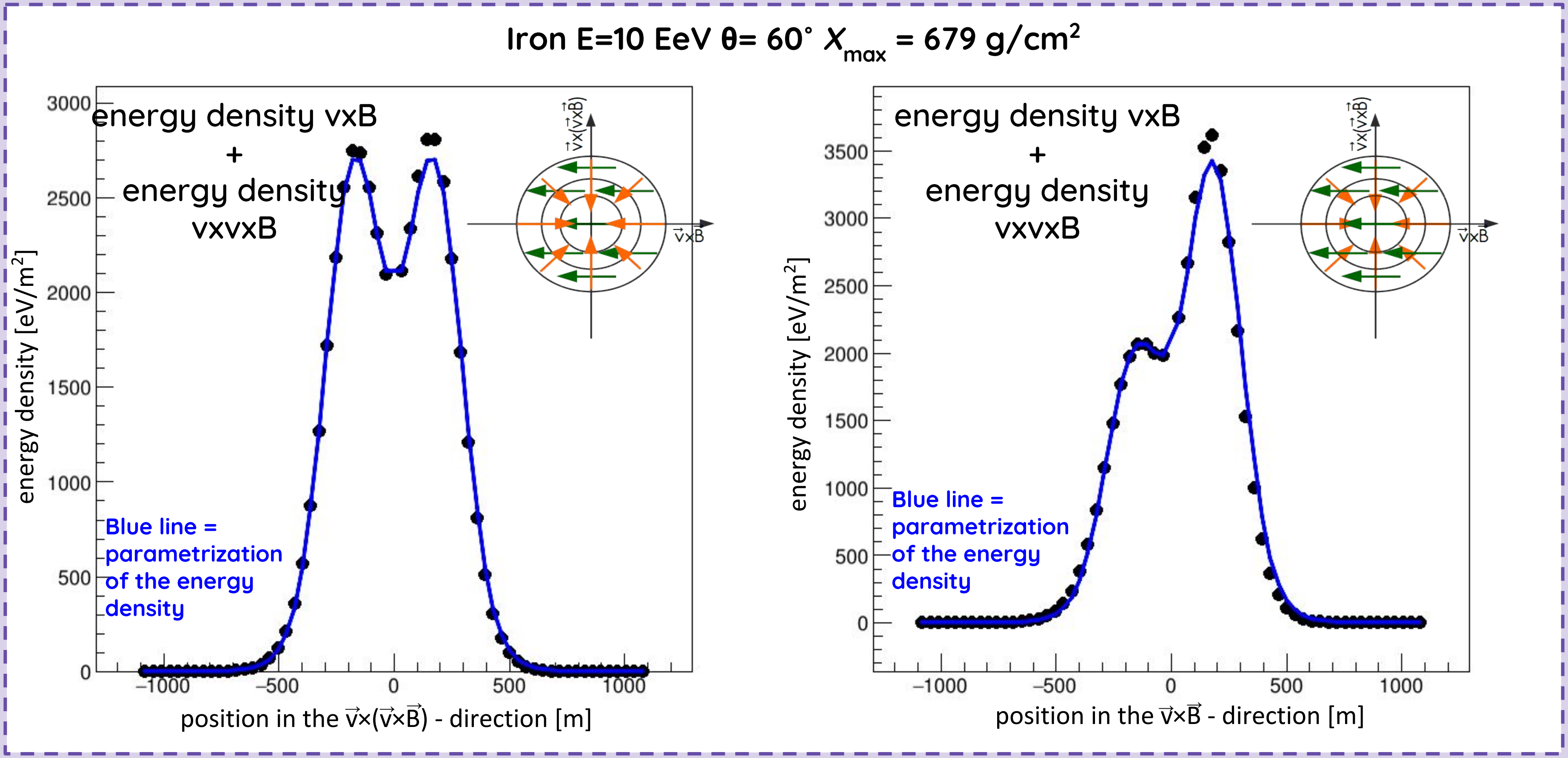

CoREAS simulation with a star-shaped antenna alignment in the shower plane $\vec{v}\times\vec{B}$-$\vec{v}\times\vec{v}\times\vec{B}$

Xmax from the energy density footprint

1.

Auger FD-RD hybrid data

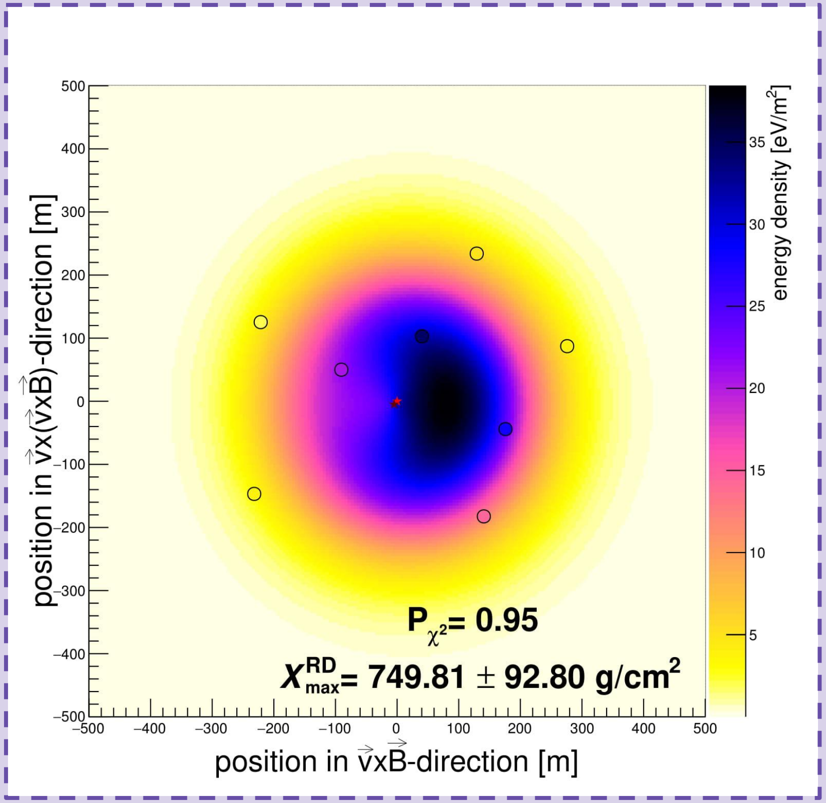

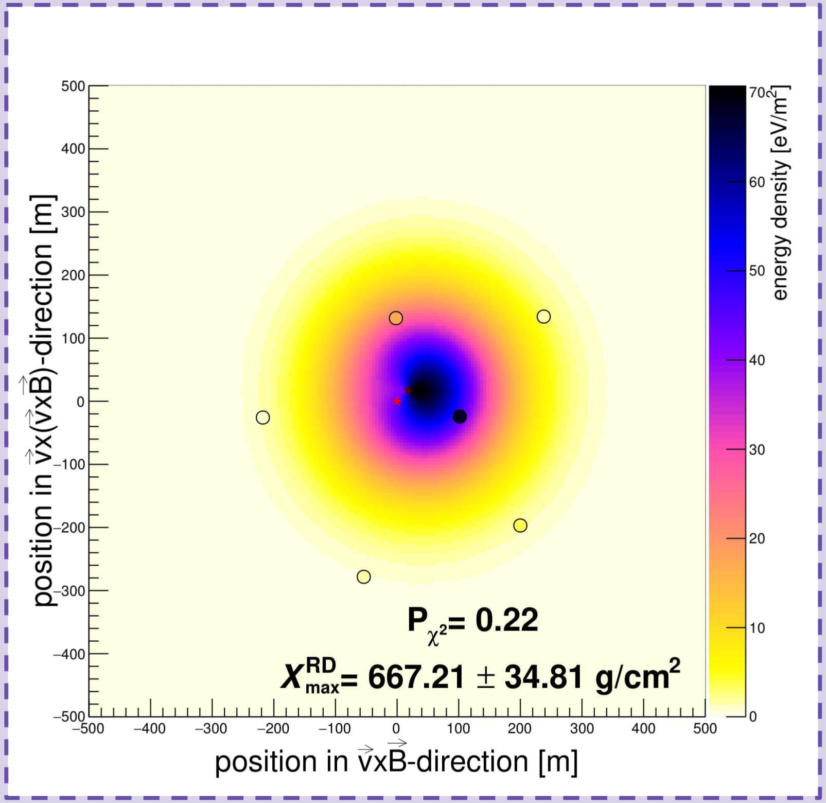

$E_{FD}=(5.45\pm0.24)\cdot10^{17}$eV

$\theta_{FD}=(50.7\pm0.2)^{\circ}$

$X_{max}^{FD}=(700.10\pm16.56)$g/cm^2

$E_{FD}=(4.78\pm0.18)\cdot10^{17}$eV

$\theta_{FD}=(41.0\pm0.2)^{\circ}$

$X_{max}^{FD}=(701.66\pm12.54)$g/cm^2

Xmax from the spectral information

2.

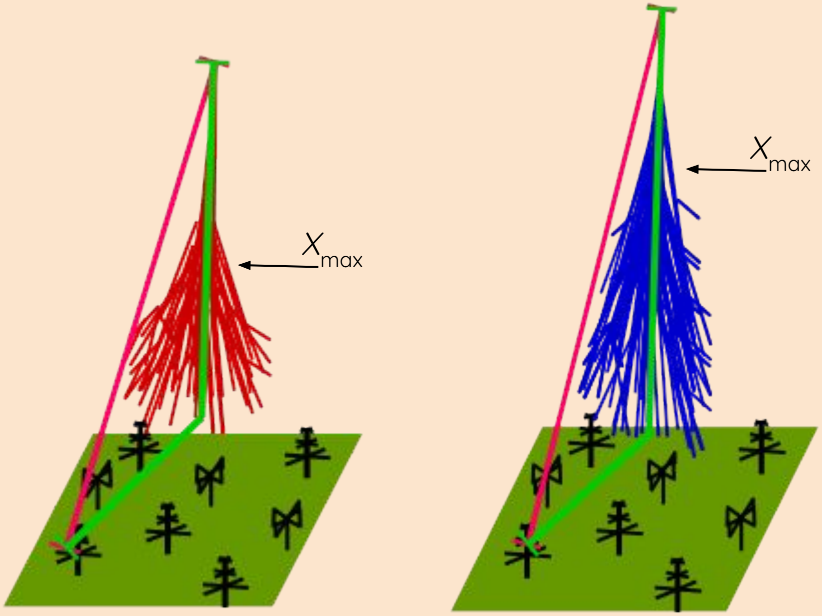

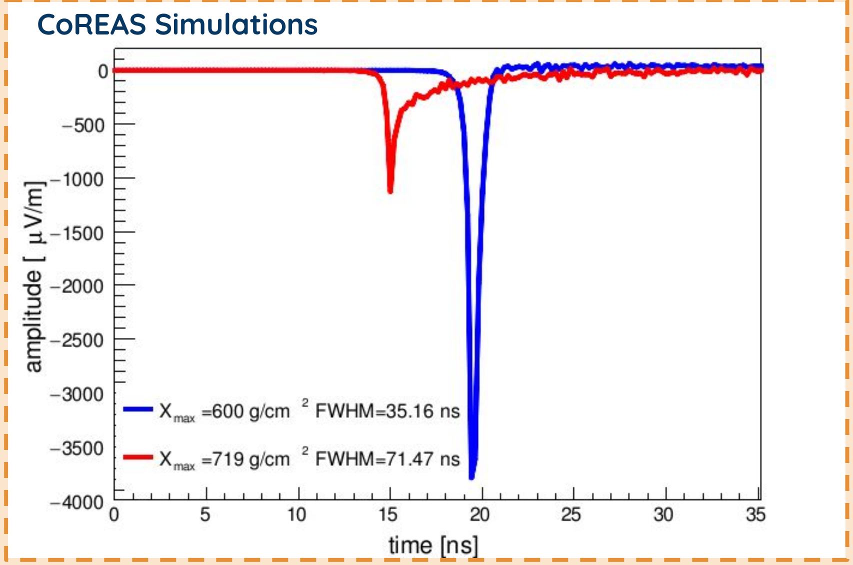

The spectral slope b depends on X_{max}

b parametrization as function of
- distance to X_{max}
- distance antenna shower axis
- angle between the antenna and the $\vec{V}\times\vec{B}$ axis

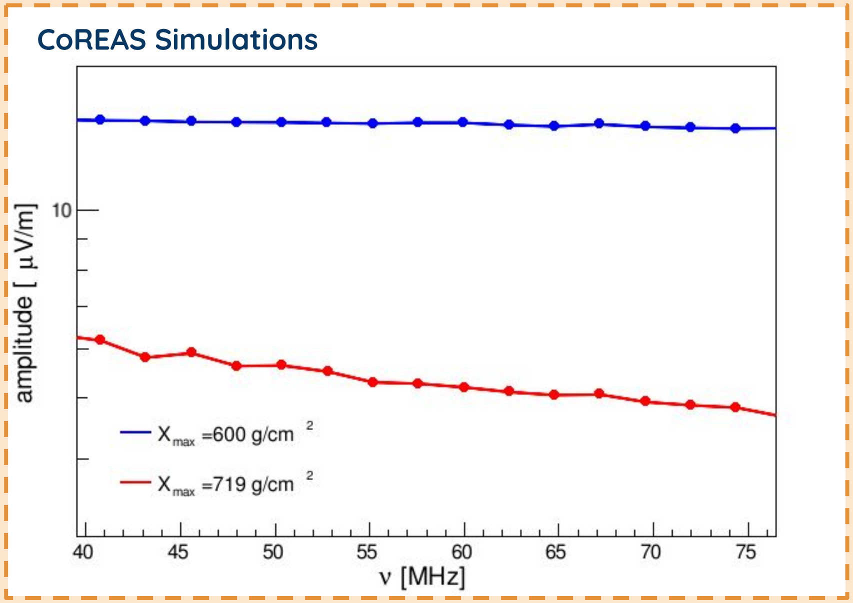

Xmax from the spectral information

2.

FD-RD X_{max} comparison for 3 events

Spectral index ***b*** as function of the the distance to the shower maximum
The **grey** line is the best prediction line obtained using X^{FD}_{max}

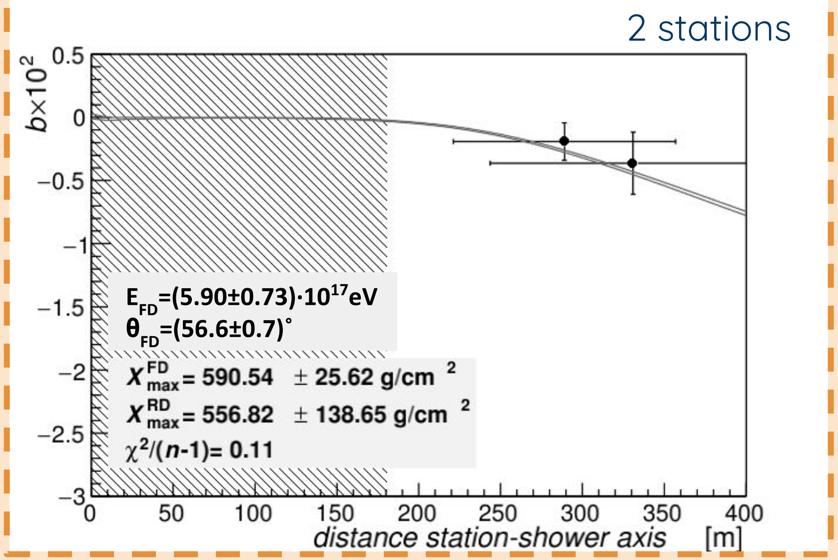

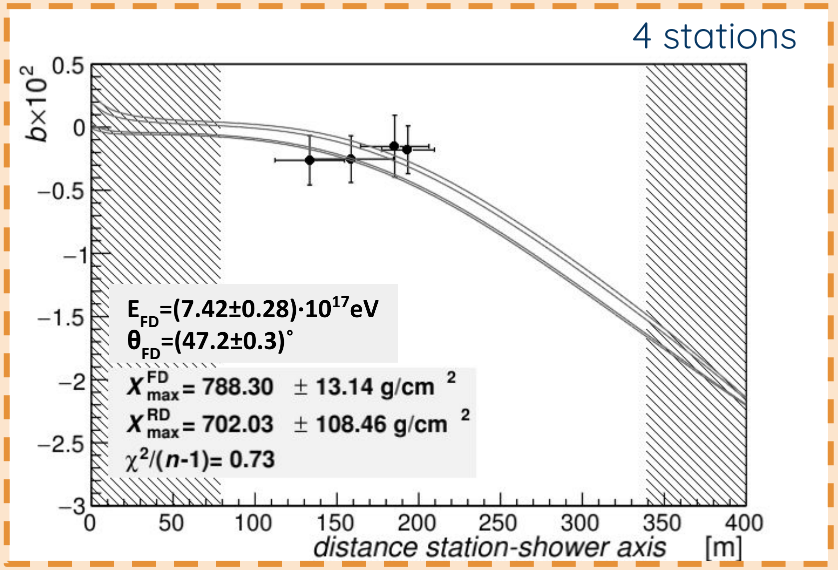

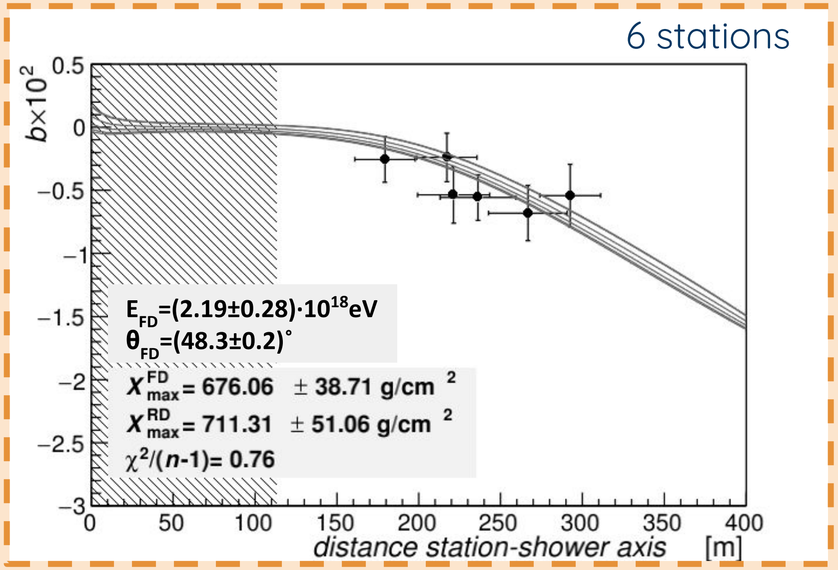

Summary

Two independent methods under investigations

1. **X_{max} from the energy density footprint**

The shape of the footprint is correlated to the distance to X_{max}.

Footprint parametrizations:

geomagnetic and charge excess mechanisms

2. **X_{max} from spectral information**

The spectral slope of radio signals depends on X_{max}.

Cosmic rays that interact high in the atmosphere have a shorter pulse and a lower spectral slope.

The results of these analysis can be combined to obtain a mass composition reconstruction that uses all the information in the detected radio signal

Backup

The Auger Engineering Radio Array

- **153** radio **antenna stations** spread over **17 km²** in the Argentinean pampa
- Sensitive to the frequency range of **30 to 80 MHz**
- Located within the **particle detector array** and in the field of view of **fluorescence telescopes** of the Pierre Auger Observatory

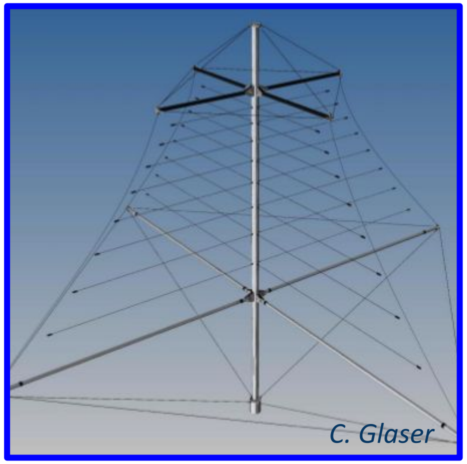

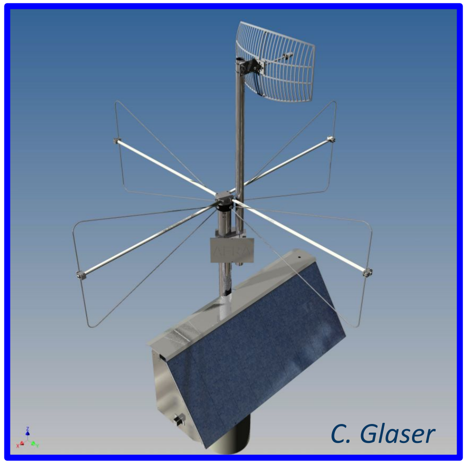

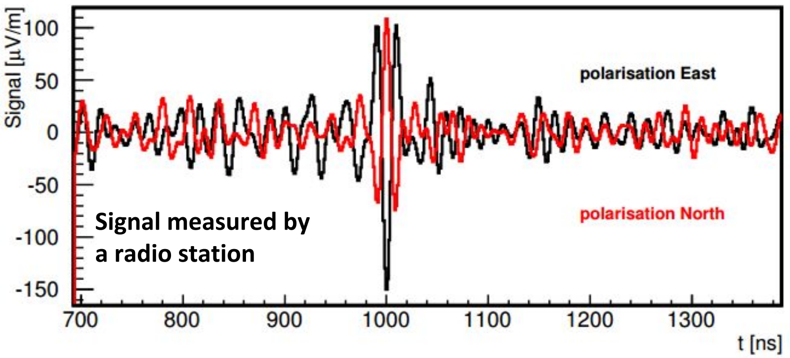

Energy density

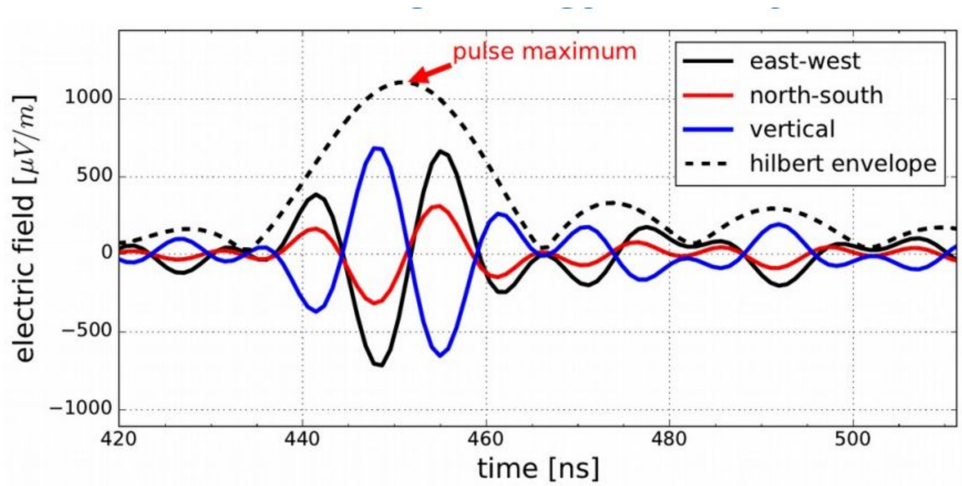

Energy density in eV/m²

Time integral of Poynting vector

$$u = \varepsilon_0 c \left(\Delta t \sum_{t_1}^{t_2} |\vec{E}(t_i)|^2 - \Delta t \frac{t_2 - t_1}{t_4 - t_3} \sum_{t_3}^{t_4} |\vec{E}(t_i)|^2 \right)$$

Window $[t_1$-$t_2]$ around the maximum of the Hilbert envelope

Noise subtraction

1.b

Parametrization of the energy density distribution:

b. description of the geomagnetic and charge excess mechanisms

Geomagnetic

$$f_{\mathrm{geo}} = \begin{cases} \frac{1}{N_{R_-}} E'_{\mathrm{geo}} \exp\left(-\left(\frac{r-R_{\mathrm{geo}}}{\sqrt{2}\sigma_{\mathrm{geo}}}\right)^{p(r)}\right) & \text{if } R_{\mathrm{geo}} < 0 \\ \frac{1}{N_{R_+}} E'_{\mathrm{geo}} \left[\exp\left(-\left(\frac{r-R_{\mathrm{geo}}}{\sqrt{2}\sigma_{\mathrm{geo}}}\right)^{p(r)}\right) + \exp\left(-\left(\frac{r+R_{\mathrm{geo}}}{\sqrt{2}\sigma_{\mathrm{geo}}}\right)^{p(r)}\right)\right] & \text{if } R_{\mathrm{geo}} \geq 0 \end{cases}$$

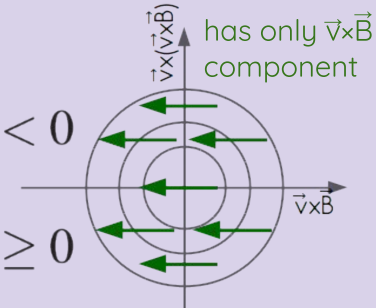

Charge excess

$$f_{\mathrm{ce}}(r) = \frac{1}{N_{\mathrm{ce}}} E'_{\mathrm{ce}}\, r^k \exp\left(\frac{-r^{p(r)}(k+1)}{p(r)\sigma_{\mathrm{ce}}^{p(r)}}\right)$$

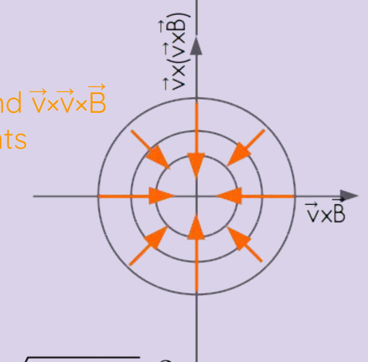

Total energy density

$$f = f_{(\vec{v}\times\vec{B})} + f_{\vec{v}\times(\vec{v}\times\vec{B})} \begin{cases} f_{\vec{v}\times\vec{B}} = \left(\sqrt{\boxed{f_{geo}(r)}} + \cos\phi\,\sqrt{\boxed{f_{ce}(r)}}\right)^2 \\ f_{\vec{v}\times(\vec{v}\times\vec{B})} = \sin^2\phi\,\boxed{f_{ce}(r)} \\ \phi = \arctan 2(y, x) \end{cases}$$

Xmax from the energy density footprint

1.b

Parametrization of the energy density distribution:

b. description of the geomagnetic and charge excess mechanisms

Polarization — **Energy density distribution**

CoREAS Simulations
Iron
E= 1.24 EeV X_{max}=679.03 g/cm^2

Geomagnetic

has only $\vec{v}\times\vec{B}$ component

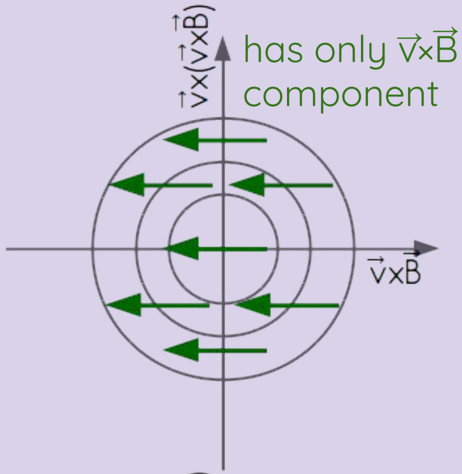

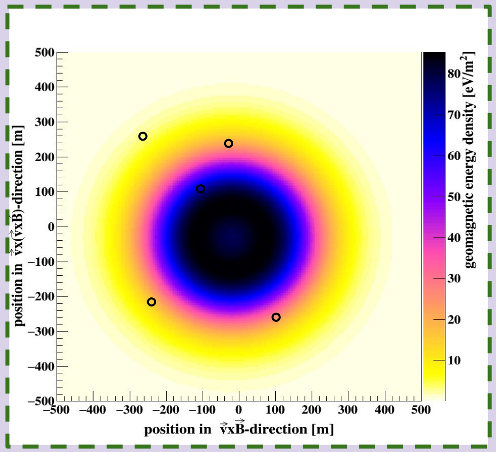

Charge excess

has $\vec{v}\times\vec{B}$ and $\vec{v}\times\vec{v}\times\vec{B}$ components

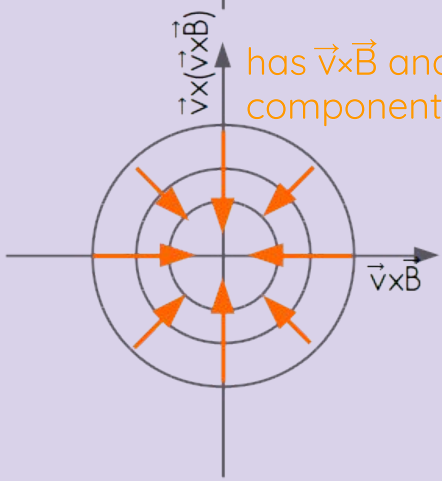

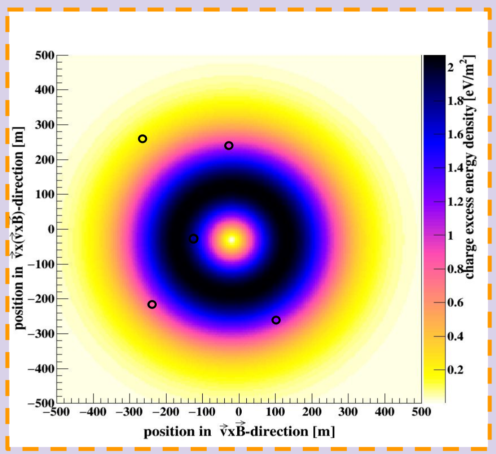

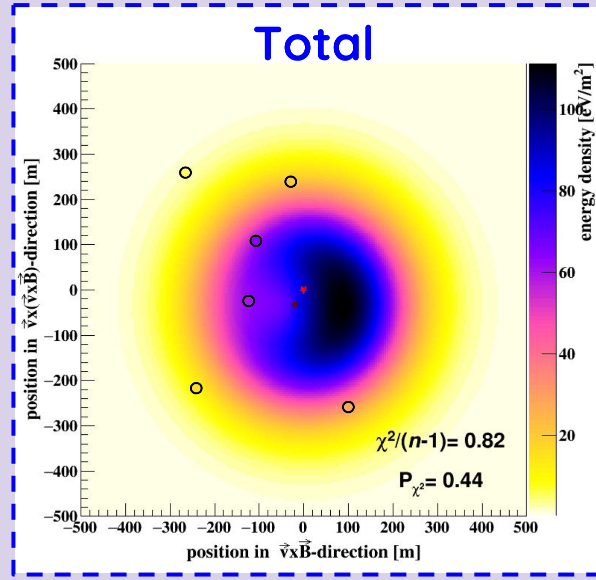

Xmax from the energy density footprint

1.a

Parametrization of the energy density distribution:

b. description of the geomagnetic and charge excess mechanisms

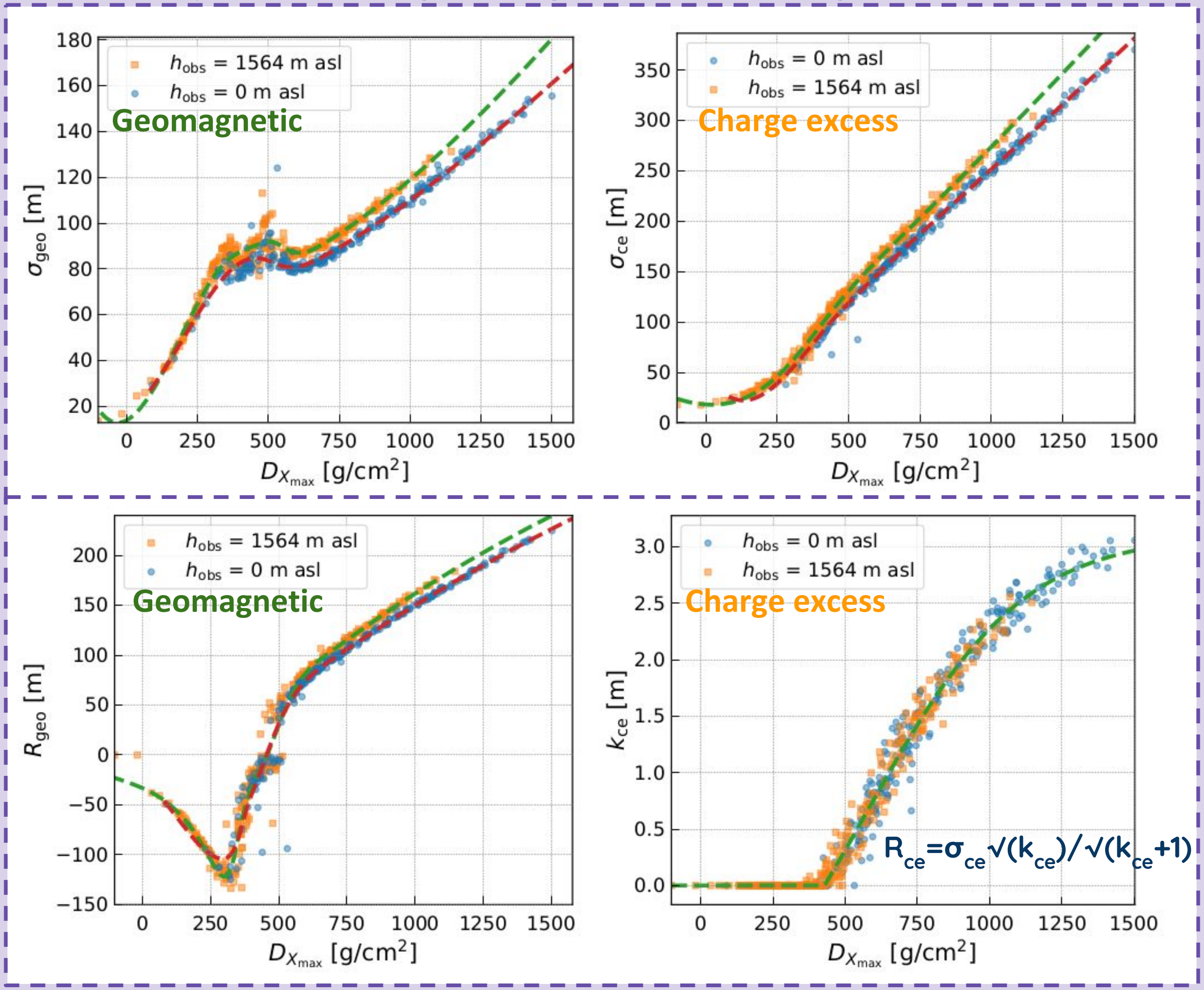

C. Glaser
arXiv:1806.03620 [astro_ph.HE]

Shape of the energy density distribution

1.b

Parametrization of the energy density distribution:

b. description of the geomagnetic and charge excess mechanisms

(A) that hit ground before emitting most radiation energy

(B) that hit ground shortly after emitting all radiation energy

(C) that have large distances between the ground and the air-shower development

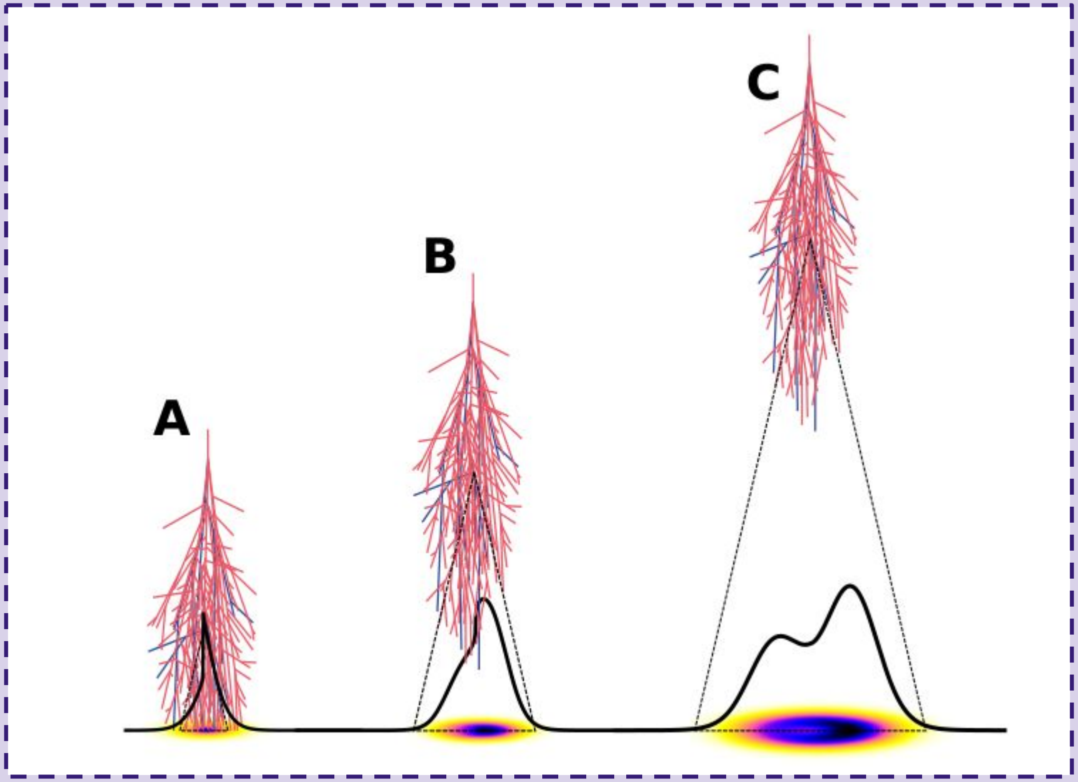

C. Glaser
arXiv:1806.03620
[astro_ph.HE]

X_{max} from the energy density footprint

1

Parametrization of the energy density distribution:

description of the geomagnetic and charge excess mechanisms

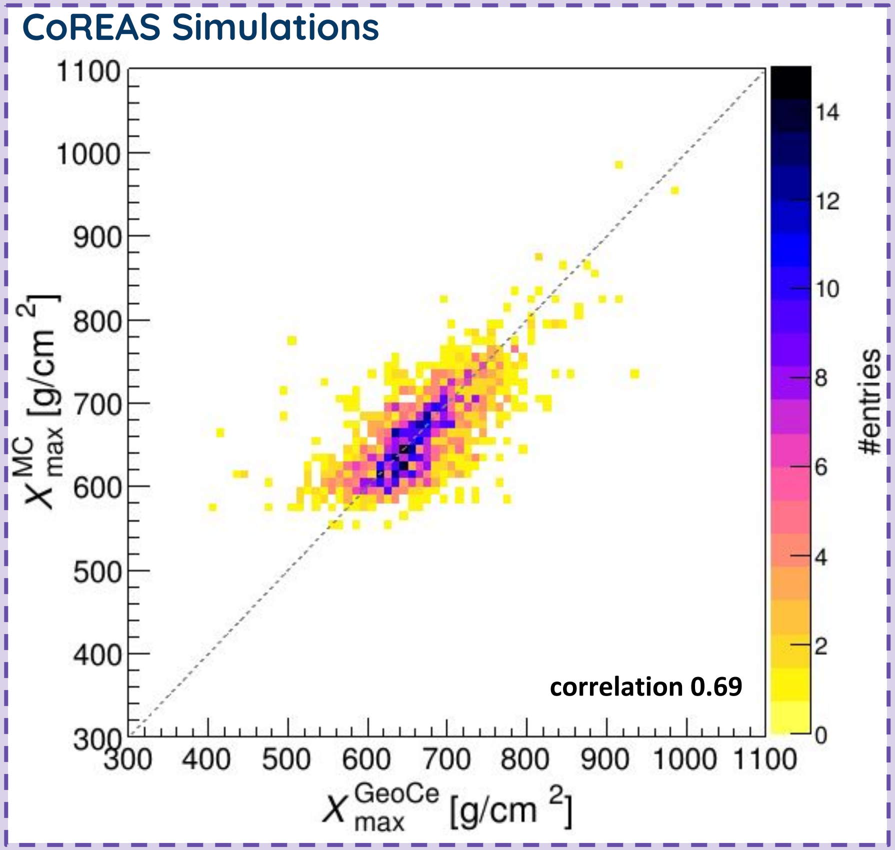

Reconstruction uncertainty ~ 41 g/cm^2

Spectral index parametrization

2.

$$b_T = \frac{1}{\nu_+ - \nu_-} \log_{10}\left[\frac{10^{b_G(\nu_+ - \nu_0)} + f(\Phi_{obs})R \cdot 10^{b_C(\nu_+ - \nu_0)}}{10^{b_G(\nu_- - \nu_0)} + f(\Phi_{obs})R \cdot 10^{b_C(\nu_- - \nu_0)}}\right]$$

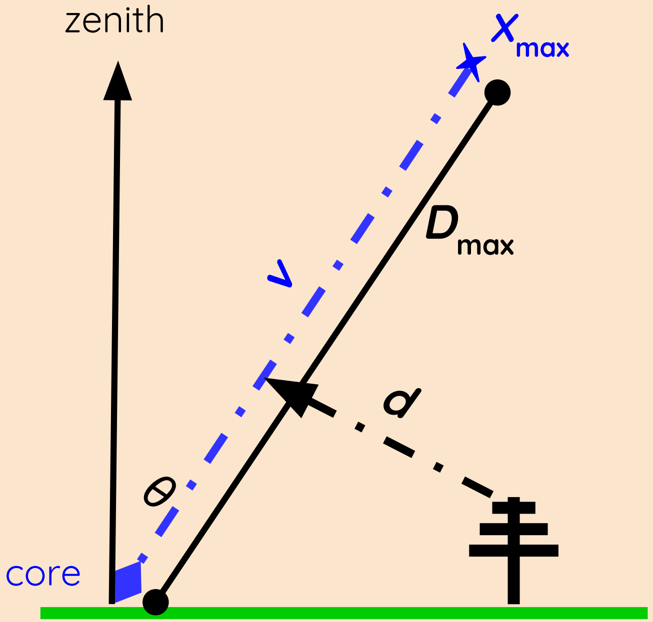

where $\boldsymbol{b_G}$ and $\boldsymbol{b_C}$:

$$b \times 10^2 = \frac{\beta}{1 + \exp(-\gamma \cdot D_{max}/1\text{km})} - \beta$$

$\boldsymbol{\beta}$ and $\boldsymbol{\gamma}$ are functions of the distance to the shower axis d

$\boldsymbol{R}$ is the ratio between the scale parameter A_C/A_G

$\boldsymbol{f(\Phi_{obs}) = \cos\Phi_{obs}}$ in the $\vec{v} \times \vec{B}$ direction

Spectral index parametrization

2.

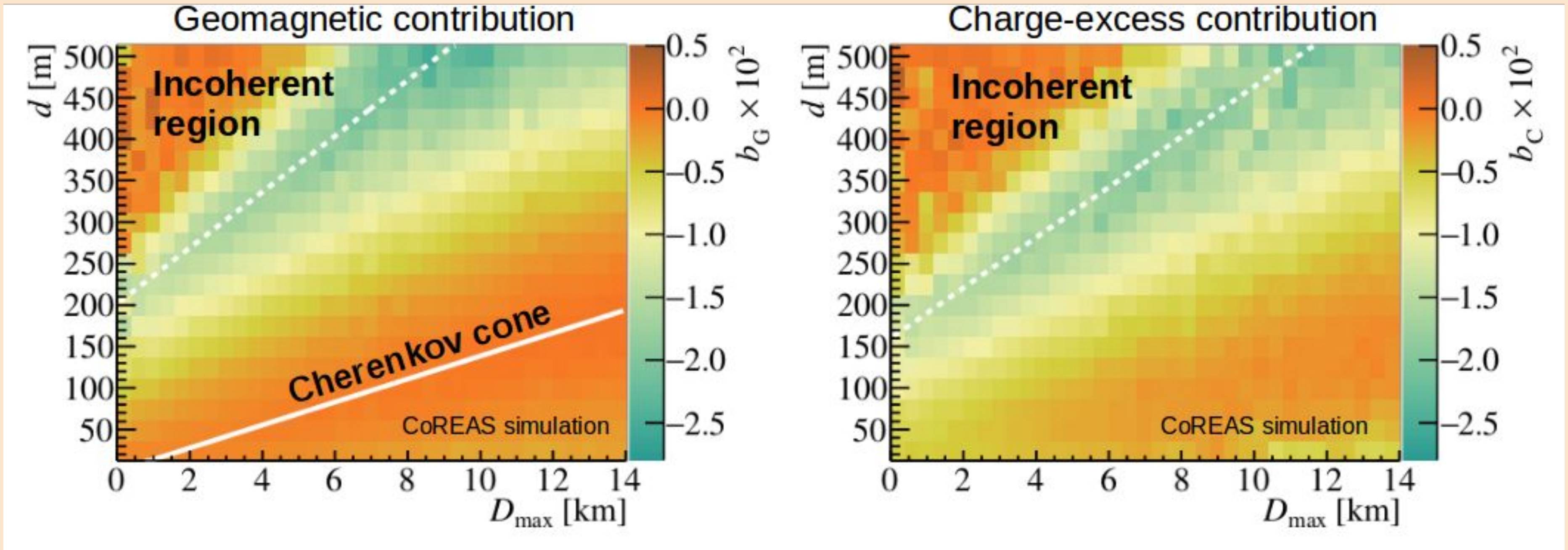

S. Jansen PhD thesis (2016)